International Journal of Thermal Sciences 49 (2010) 10–22

Contents lists available at ScienceDirect

International Journal of Thermal Sciences

journal homepage: www.elsevier.com/locate/ijts

Application of integral transform technique to the transient laminar flow heat transfer in the ducts

A. Hadiouche, K. Mansouri*

University M. Bougara of Boumerdes, Faculty of Engineering Science, Department of Energy, Boumerdes 35000, Algeria

ARTICLE INFO

Article history:
Received 18 June 2008
Received in revised form
1 April 2009
Accepted 26 May 2009
Available online 1 July 2009

Keywords:
Conjugated forced convection
Laminar flow
Periodic inlet temperature
Quasi-steady model
Analytical solution

ABSTRACT

In this paper, a theoretical study of laminar forced convection inside ducts, subjected to periodically varying inlet temperature is presented. A thermal diffusion in the duct walls and a boundary condition which accounts for external convection are considered. In the first part, this problem is solved by applying a Generalized Integral Transform Technique (GITT). The complex eigenvalues and coefficients results are listed and compared with the literature. In the second part, the Quasi-steady Approach (QSA) which employs a constant heat transfer coefficient at liquid–solid interface is also investigated and compared with the GITT solution. The bulk temperature, Nusselt number, the damping and phase lag coefficients as function of the inlet temperature frequency are plotted.

1. Introduction

Knowledge of the thermal response of the duct wall and the fluid temperature subjected to a periodic disturbance applied at the inlet in forced laminar and turbulent flow inside ducts is important for many engineering applications, where hot and cold fluids pass in succession, such as in regenerative and recuperative heat exchangers.

The investigations on forced convection with periodic inlet temperature have been performed by numerous researchers [1–18]. The solution of heat transfer problems of this type usually leads to a non classical Sturm–Liouville complex system which no known solutions are available. The main difficulty in the analysis of this class of problems is finding the solution for the resulting complex eigenvalue problem.

In the studies [1–6], only the fluid energy equation was solved but without conjugation with the walls. Kakaç and Yener [1,2] considered a transient energy equation with inlet temperature varying over time for slug flow and turbulent heat transfer between two parallel-plates. The resulting Sturm–Liouville problem could not be solved and an experimental technique was utilized to estimate the first eigenvalue. Cotta and Ozisik [3] studied laminar forced convection with periodic variations of inlet temperature without conjugation with the walls both parallel-plate and circular ducts. They used an integral transform technique, avoiding the complex eigenvalue problem and solving a coupled system of ordinary differential equations.

In references [7–16], the methodologies used in the previous works are advanced further by considering the effects of heat capacity of a duct wall. Sparrow and Farias [7] seem to be the first investigators who included the effect of wall conjugation. They investigated the slug flow periodic laminar forced convection in a parallel-plate channel but without considering the effects of heat conduction within the wall. A trial and error procedure was employed for the numerical evaluation of the real and imaginary parts of the complex eigenvalues. Cotta et al. [8] utilized the solution methodology suggested by Sparrow and Farias [7] to solve the conjugated laminar forced convection in parallel-plate ducts and circular tubes for slug flow with periodically varying inlet temperature. The sign-Count modifying method is adopted for the determination of the complex eigenvalues. Kim and Ozisik [9] treated the same problem with parabolic velocity profile, the resulting complex eigenvalues problem is solved by using a Runge–Kutta method. Travelho and Santos [10,11] solved the same problem that had been developed before in ref. [7,8] with the same physical conditions by applying the Laplace transform, avoiding the computation of the complex eigenvalues and numerically calculating the inverse of the Laplace transform. Kakaç and Li [12,13] recalled the theoretical analysis of [1] to add the effects of wall thermal capacitance and external convection but still without conduction within the wall.

* Corresponding author. Tel./fax: +(213) 024 81 93 95.
E-mail address: manskac@yahoo.fr (K. Mansouri).

1290-0729/$ – see front matter
doi:10.1016/j.ijthermalsci.2009.05.012

Nomenclature

a_{nk}	coefficient defined by equation (9b)
a^+	fluid-to-wall thermal capacitance ratio $[\rho_f C_f R_1/\rho_s C_s(R_2-R_1)]$
$A(x^+)$	dimensionless temperature amplitude
b_{nk}	coefficient, defined by equation (9b)
Bi_{ext}	external Biot number $[h_{ext}R_1/k_f]$
Bi_{int}	internal Biot number $[h_{int}R_1/k_f]$
Bi^+	modified Biot number $[h_{ext}R_1/k_f]$
C_n	coefficient, defined by equation (11b)
$\bar{f}_n$	coefficient defined by equation (11c)
h_{ext}	convection heat transfer coefficient outside the wall ($W\,m^{-2}\,K^{-1}$)
h_{int}	convection heat transfer coefficient inside the wall ($W\,m^{-2}\,K^{-1}$)
k	thermal conductivity ($W\,m^{-1}\,K^{-1}$)
q_w	wall heat flux
r	radial or normal coordinate (m)
R_1	radius of circular duct or half the spacing between parallel-plate (m)
R_2	outer radius (m)
T	fluid temperature (K)
T_∞	ambient temperature (K)
T_0	amplitude of inlet temperature (K)
t	time variable (s)
u	flow velocity ($m\,s^{-1}$)
$\bar{u}$	mean velocity ($m\,s^{-1}$)
v_{nk}	eigenvector for equation (10)
x	axial coordinate (m)

Greek symbols

α	thermal diffusivity ($m^2\,s^{-1}$)
β	$(R_2-R_1)\sqrt{\omega/2\alpha_s}$
Ω	dimensionless inlet frequency
μ_n	eigenvalues of equation (10)
η	damping coefficient
$\varphi(x^+)$	phase lag (Rad)
θ	solid temperature (K)
τ	period $[2\pi/\omega]$ (s)
ω	inlet frequency (Hz)

Subscripts and superscripts

b	bulk temperature
c, w	centreline and wall value
f, s	fluid and solid properties

In [14] a periodic laminar forced convection within the thermal entrance region of parallel-plate channels is analytically solved by making use of the Generalized Integral Transform Technique (GITT) and mixed symbolic-numerical computation. A fifth kind boundary condition at the channel walls that includes external convection and wall thermal capacitance effects is considered.

The same problem, which takes into account the heat axial diffusion along the duct wall, is investigated by Guedes and Cotta [15] and Guedes et al [16]. A "thin wall" model is adopted that neglects transversal temperature gradients in the solid.

In the studies [7–16], the wall effects are included in the thermal boundary condition at the fluid–wall interface. This condition can be justified only for heat transfer in flows bounded by extremely thin walls. In general case, the channel wall has a finite thickness and thermal capacitance. To study this problem deeply, it is necessary to take in consideration the heat conduction in the wall. Fourcher and Mansouri [17,18] analysed the problem of periodic laminar and turbulent forced convection taking into account the transversal heat conduction in the duct walls.

There exist other studies on the extensions to the Graetz problem. Among the important extensions are the consideration of slip flow [19–21], non Newtonian fluids [22,23] and viscous dissipation [24]. In the literature, only a limited amount of works is available on conjugate heat transfer problems with heat diffusion in the duct walls. This is the reason why, in this work, the transversal heat conduction in duct walls is considered in the analytical solution of the periodic laminar forced convection inside ducts. A parabolic velocity profile and convection from the ambient medium are accounted. An appropriate extension of the Generalized Integral Transform Technique (GITT) is developed, avoiding the complex eigenvalue system and solving a coupled first-order ordinary differential equations. This technique constitutes a complete solution (CS) of the conjugated periodic problem.

For most engineering applications, the thermal design engineer reduces considerably the theoretical analysis by using the quasi-steady approach (QSA) which employs a standard heat transfer coefficient at fluid–solid interface. Consequently, the question which can be put is to know the limits of such approach in its capacity of prediction. In this work, it was decided to compare it to the complete solution (CS). The effects of the dimensionless frequency of inlet oscillations on the damping and phase lag coefficients are illustrated.

2. Problem formulation

Consider laminar forced convection inside ducts, such as parallel-plate channels and circular tubes, subjected to periodic time variation in the inlet temperature as represented in Fig. 1. The transversal heat conduction within the duct walls is considered.

The dimensionless formulation of this transient conjugated problem is given as:

Fluid region

$$\frac{\partial T^+}{\partial t^+}+u^+\left(r^+\right)\frac{\partial T^+}{\partial x^+}=\frac{1}{r^{+m}}\frac{\partial}{\partial r^+}\left(r^{+m}\frac{\partial T^+}{\partial r^+}\right)$$
$$0<r^+<1;\ x^+>0;\ t^+>0, \tag{1a}$$

$$T^+=\sin\left(\Omega t^+\right),\quad \text{at}\quad x^+=0;\ 0\le r^+\le 1;\ t^+>0 \tag{1b}$$

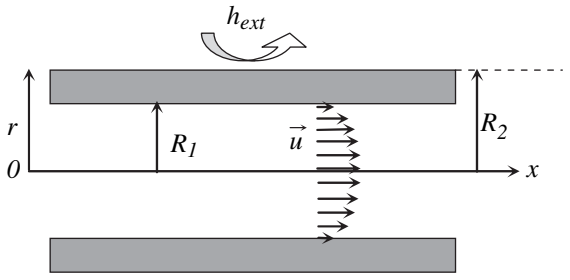

Fig. 1. Geometry of the theoretical analysis.

$$\frac{\partial T^+}{\partial r^+} = 0, \quad \text{at} \quad r^+ = 0;\ x^+ > 0;\ t^+ > 0 \tag{1c}$$

Solid region

$$\Gamma\frac{\partial \theta}{\partial t^+} = \frac{1}{r^{+m}}\frac{\partial}{\partial r^+}\left(r^{+m}\frac{\partial \theta}{\partial r^+}\right), \quad 1 < r^+ < r_2^+;\ x^+ > 0;\ t^+ > 0 \tag{1d}$$

$$-\frac{\partial \theta}{\partial r^+} = Bi_{\text{ext}}\theta, \quad \text{at} \quad r^+ = r_2^+;\ x^+ > 0;\ t^+ > 0 \tag{1e}$$

Fluid–solid interface

$$\begin{gathered}\gamma\frac{\partial \theta}{\partial r^+} = \frac{\partial T^+}{\partial r^+},\\ \theta = T^+. \quad \text{at} \quad r^+ = 1;\ x^+ > 0;\ t^+ > 0.\end{gathered} \tag{1f}$$

where $m = 0$, for parallel-plate channel and $m = 1$, for circular duct. The used dimensionless groups are given as follow:

$$r^+ = \frac{r}{R_1};\quad r_2^+ = \frac{R_2}{R_1};\quad x^+ = \frac{x\alpha_f}{R_1^2\overline{u}};\quad t^+ = \frac{t\alpha_f}{R_1^2};\quad \gamma = \frac{k_s}{k_f};$$
$$T^+ = \frac{T - T_\infty}{\Delta T};\quad \theta = \frac{T_w - T_\infty}{\Delta T};$$

$$Bi_{\text{ext}} = \frac{h_{\text{ext}}R_1}{k_s};\quad \Omega = \frac{\omega R_1^2}{\alpha_f};\quad \Gamma = \frac{\alpha_f}{\alpha_s};$$
$$\beta = (R_2 - R_1)\sqrt{\frac{\omega}{2\alpha_s}} \text{ and } u^+\left(r^+\right) = \frac{u(r)}{\overline{u}}$$

where $u^+(r^+)$ is the dimensionless velocity profile, or

$$u^+\left(r^+\right) = \begin{cases}\frac{2^m+2}{2}\left(1 - r^{+2}\right) & \text{for parabolic flow}\\ 1 & \text{for slug flow}\end{cases}$$

Here, we are interested in the periodic solution of the problem. We seek a solution as:

$$\begin{aligned}T^+(x^+, r^+, t^+) &= \tilde{T}^+(x^+, r^+)\exp(i\Omega t^+)\\ \theta(x^+, r^+, t^+) &= \tilde{\theta}(x^+, r^+)\exp(i\Omega t^+).\end{aligned} \tag{2}$$

where $i = \sqrt{-1}$. When we substitute equation (2) into equations (1), we obtain the following system:

Fluid region

$$i\Omega\tilde{T}^+ + u^+\left(r^+\right)\frac{\partial \tilde{T}^+}{\partial x^+} = \frac{1}{r^{+m}}\frac{\partial}{\partial r^+}\left(r^{+m}\frac{\partial \tilde{T}^+}{\partial r^+}\right), \ 0 < r^+ < 1; x^+ > 0 \tag{3a}$$

$$\tilde{T}^+ = 1, \ \text{at} \ x^+ = 0;\ 0 \le r^+ \le 1 \tag{3b}$$

$$\frac{\partial \tilde{T}^+}{\partial r^+} = 0 \ \text{at} \ r^+ = 0;\ x^+ > 0 \tag{3c}$$

Solid region

$$2i\left(\frac{\beta}{r_2^+ - 1}\right)^2\tilde{\theta} = \frac{1}{r^{+m}}\frac{\partial}{\partial r^+}\left(r^{+m}\frac{\partial \tilde{\theta}}{\partial r^+}\right), \quad 1 < r^+ < r_2^+;\ x^+ > 0 \tag{4a}$$

$$\frac{\partial \tilde{\theta}}{\partial r^+} = -Bi_{\text{ext}}\tilde{\theta}, \ \text{at} \ r^+ = r_2^+;\ x^+ > 0 \tag{4b}$$

Fluid–solid interface

$$\begin{gathered}\gamma\frac{\partial \tilde{\theta}}{\partial r^+} = \frac{\partial \tilde{T}^+}{\partial r^+},\\ \tilde{\theta} = \tilde{T}^+, \quad \text{at} \quad r^+ = 1;\ x^+ > 0.\end{gathered} \tag{4c}$$

3. Complete solution (CS)

Introducing the complex parameter $\tilde{\beta} = \beta(1 - i)$, the temperature distribution within the solid for both geometries of the duct is relegated to the Appendix. The fluid temperature will be found by solving the following system:

$$i\Omega\tilde{T}^+ + u^+\left(r^+\right)\frac{\partial \tilde{T}^+}{\partial x^+} = \frac{1}{r^{+m}}\frac{\partial}{\partial r^+}\left(r^{+m}\frac{\partial \tilde{T}^+}{\partial r^+}\right), \ 0 < r^+ < 1; x^+ > 0 \tag{5a}$$

$$\tilde{T}^+ = 1, \quad \text{at} \quad x^+ = 0;\ 0 \le r^+ \le 1 \tag{5b}$$

$$\frac{\partial \tilde{T}^+}{\partial r^+} = 0, \quad \text{at} \quad r^+ = 0;\ x^+ > 0 \tag{5c}$$

$$\frac{\partial \tilde{T}^+}{\partial r^+} + \tilde{H}\tilde{T}^+ = 0 \quad \text{at} \quad r^+ = 1;\ x^+ > 0. \tag{5d}$$

The complex coupling parameter $\tilde{H}$ is given for both geometries of the duct and the asymptotic cases are discussed in the appendix. It can be written in general form as:

$$\tilde{H} = R_H + iG_H. \tag{6}$$

A formal solution of the problem (5) is developed through the classical Integral Transform Technique (GITT). However, the complete numerical solution would require an accurate evaluation of eigenvalues and eigenfunctions of the corresponding complex non classical Sturm–Liouville system. To avoiding the complex eigenquantities problem, an appropriate auxiliary problem is chosen as:

$$\frac{1}{r^{+m}}\frac{\partial}{\partial r^+}\left(r^{+m}\frac{\partial \psi(\lambda, r^+)}{\partial r^+}\right) + \lambda^2\psi\left(\lambda, r^+\right) = 0, \quad 0 < r^+ < 1 \tag{7a}$$

$$\frac{\partial \psi(\lambda, r^+)}{\partial r^+} = 0, \quad \text{at} \quad r^+ = 0 \tag{7b}$$

$$\frac{\partial \psi(\lambda, r^+)}{\partial r^+} + R_H\psi\left(\lambda, r^+\right) = 0, \quad \text{at} \quad r^+ = 1. \tag{7c}$$

The eigenfunctions of the auxiliary problem are given respectively for parallel-plate channel and circular ducts by:

$\psi_n(r^+) = \cos(\lambda_n r^+)$ and $\psi_n(r^+) = J_0(\lambda_n r^+)$, while the related parameter λ can be determined respectively by the following transcendental equations: $\lambda_n tg(\lambda_n) = R_H$ and $R_H J_0(\lambda_n) = \lambda_n J_1(\lambda_n)$.

The auxiliary problem (7) allows the definition of an integral transform pair for the function $\tilde{T}^+(x^+, r^+)$ given by:

$$\text{Inversion} \quad \tilde{T}^+\left(x^+, r^+\right) = \sum_{n=1}^{\infty}\frac{\psi_n(r^+)}{\sqrt{N_n}}\overline{\tilde{T}}_n^+\left(x^+\right) \tag{8a}$$

$$\text{Transform} \quad \overline{\tilde{T}}_n^+\left(x^+\right) = \int_0^1\frac{\psi_n(r^+)}{\sqrt{N_n}}\tilde{T}^+\left(x^+, r^+\right)r^{+m}\mathrm{d}r^+ \tag{8b}$$

where the normalization integral is given by

$$N_n = \int_0^1 \left[\psi_n(r^+)\right]^2 r^{+m}\mathrm{d}r^+. \tag{8c}$$

Equation (5a) and inlet condition (5b) are now operated by:

$$\int_0^1 \frac{\psi_n(r^+)}{\sqrt{N_n}} r^{+m}\mathrm{d}r^+. \tag{8d}$$

By applying the inversion formula (8a), we obtain the following equations:

$$\sum_{n=1}^{\infty} a_{nk}\frac{\mathrm{d}\bar{\tilde{T}}_k^+(x^+)}{\mathrm{d}x^+} + \sum_{n=1}^{\infty} b_{nk}\bar{\tilde{T}}_k^+\left(x^+\right) = 0, \quad x^+ > 0 \tag{9a}$$

where, $a_{nk} = \int_0^1 r^{+m}u^+(r^+)\frac{\psi_n(r^+)\psi_k(r^+)}{\sqrt{N_n}\sqrt{N_k}}\mathrm{d}r^+$ and

$$b_{nk} = \delta_{nk}\lambda_n^2 + i\left[\delta_{nk}\Omega + G_H\frac{\psi_n(1)\psi_k(1)}{\sqrt{N_n}\sqrt{N_k}}\right] \tag{9b}$$

The system (9) forms a set of infinite, coupled, first-order linear ordinary differential equations. Usually, it is very difficult to solve analytically the problem. Therefore, taking a sufficiently large number of equations, N, the system (9) can be expressed in matrix form as:

$$[b_{nk} - \mu a_{nk}]v_{nk.} = 0. \tag{10}$$

Once the related problem (10) is solved for the eigenvalues μ_n and eigenvectors v_{nk}, the solution is constructed from the linear combination of independent solutions:

$$\bar{\tilde{T}}_n^+\left(x^+\right) = \sum_{k=1}^{N} C_k v_{nk}\exp\left(-\mu_k x^+\right), \tag{11a}$$

where v_{nk} is the kth component of the nth eigenvector and C_k are determined by using this solution to satisfy the inlet condition,

$$\sum_{k=1}^{N} C_k v_{nk} = \bar{f}_n. \tag{11b}$$

$$\text{where } \bar{f}_n = \int_0^1 r^{+m}\frac{\psi_n(r^+)}{\sqrt{N_n}}\mathrm{d}r^+ \tag{11c}$$

Then, the inversion formula given by equation (8a) is invoked to compute the complete solution:

$$\tilde{T}^+\left(x^+, r^+\right) = \sum_{n=1}^{N}\frac{\psi_n(r^+)}{\sqrt{N_n}}\sum_{k=1}^{N} C_k v_{nk}\exp\left(-\mu_k x^+\right). \tag{12a}$$

At the centreline of the duct, equation (12a) can be written as:

$$\begin{aligned}\tilde{T}_c^+\left(x^+\right) &= \sum_{n=1}^{N}\frac{\psi_n(0)}{\sqrt{N_n}}\sum_{k=1}^{N} C_k v_{nk}\exp\left(-\mu_k x^+\right)\\ &= \sum_{k=1}^{N} C_k\exp\left(-\mu_k x^+\right)\sum_{n=1}^{N}\frac{v_{nk}}{\sqrt{N_n}}\\ &= \sum_{k=1}^{N} G_k\exp\left(-\mu_k x^+\right)\end{aligned} \tag{12b}$$

where $G_k = C_K\sum_{n=1}^{N}\frac{v_{nk}}{\sqrt{N_n}}$.

We determine the dimensionless wall heat flux, wall and bulk temperature respectively $\tilde{q}_w(x^+)$, $\tilde{T}_w(x^+)$ and $\tilde{T}_b(x^+)$ from their definitions:

$$\begin{aligned}\tilde{q}_w\left(x^+\right) &= -\left.\frac{\partial\tilde{T}^+}{\partial r^+}\right|_{r^+=1} = -\sum_{k=1}^{N} C_k\exp\left(-\mu_k x^+\right)\sum_{n=1}^{N}\frac{v_{nk}}{\sqrt{N_n}}\psi_n'(1)\\ &= \sum_{k=1}^{N} Q_k\exp\left(-\mu_k x^+\right)\end{aligned} \tag{13a}$$

$$\begin{aligned}\tilde{T}_w\left(x^+\right) &= \sum_{k=1}^{N} C_k\exp\left(-\mu_k x^+\right)\sum_{n=1}^{N}\frac{v_{nk}}{\sqrt{N_n}}\psi_n(1)\\ &= \sum_{k=1}^{N} W_k\exp\left(-\mu_k x^+\right),\end{aligned} \tag{13b}$$

$$\begin{aligned}\tilde{T}_b\left(x^+\right) &= (m+1)\int_0^1 r^{+m}u^+\left(r^+\right)\tilde{T}^+\left(x^+, r^+\right)\mathrm{d}r^+\\ &= \sum_{k=1}^{N} M_k\exp\left(-\mu_k x^+\right),\end{aligned} \tag{13c}$$

where $Q_k = -C_k\sum_{n=1}^{N}\frac{v_{nk}}{\sqrt{N_n}}\psi_n'(1)$; $W_k = C_k\sum_{n=1}^{N}\frac{v_{nk}}{\sqrt{N_n}}\psi_n(1)$

$$\text{and } M_k = (m+1)C_k\sum_{n=1}^{N}\frac{v_{nk}}{\sqrt{N_n}}\int_0^1 r^{+m}u^+\left(r^+\right)\psi_n\left(r^+\right)\mathrm{d}r^+. \tag{13d}$$

So, the final solutions can be conveniently expressed in polar coordinates as:

$$q_w\left(x^+, t^+\right) = A_f\left(x^+\right)\sin\left[\Omega t^+ - \phi_f\left(x^+\right)\right], \tag{14a}$$

$$T_{c,w,b}^+\left(x^+, t^+\right) = A_{c,w,b}\left(x^+\right)\sin\left[\Omega t^+ - \phi_{c,w,b}\left(x^+\right)\right], \tag{14b}$$

$$\text{where } A_f\left(x^+\right) = \left|q_w\left(x^+\right)\right| \text{ and } \phi_f\left(x^+\right) = -\arg q_w\left(x^+\right), \tag{14c}$$

$$A_{c,w,b}\left(x^+\right) = \left|\tilde{T}_{c,w,b}^+\left(x^+\right)\right| \text{ and } \phi_{c,w,b}\left(x^+\right) = -\arg\tilde{T}_{c,w,b}^+\left(x^+\right).$$

We determine the Nusselt number Nu from its definition:

$$Nu\left(x^+, t^+\right) = 2^{2-m}\frac{\left.\frac{\partial T^+(r^+, x^+, t^+)}{\partial r^+}\right|_{r^+=1}}{\theta(1, x^+, t^+) - T_b^+(x^+, t^+)}. \tag{15}$$

4. Quasi-steady approach (QSA)

For comparison purpose, the same problem (1) will also be solved by the quasi-steady approach (QSA) which uses a constant heat transfer coefficient at liquid–solid interface. The problem will now be analyzed under the assumption of the heat flux:

$$q_w = -\frac{\partial T^+}{\partial r^+} = h_{int}\left(T_b^+ - \theta\right) \quad \text{at} \quad r^+ = 1;\ x^+ > 0;\ t^+ > 0 \tag{16}$$

where q_w, T_b^+ and θ are function of time, but h_{int} is time independent. In applying the quasi-steady model, the problem consists to determine the bulk temperature T_b^+, which is defined as:

$$T_b^+\left(x^+\right) = (m+1)\int_0^1 r^{+m}u^+\left(r^+\right)T^+\left(x^+, r^+\right)\mathrm{d}r^+ \tag{17}$$

Table 1
The first five coefficients and eigenvalues for a parallel-plate channel for different a^+ at $Bi_{ext} = 0.0$ and $\Omega = 0.1$.

a^+	n	λ_n	μ_n	G_n
5E−5	1	0.14928E+1	0.17982E+1+0.17087E+0i	0.11965E+1+0.64585E−2i
	2	0.44819E+1	0.20770E+2+0.78869E+0i	−0.29048E+0−0.11147E−1i
	3	0.74807E+1	0.60701E+2+0.17334E+1i	0.15330E+0+0.96730E−2i
	4	0.10493E+2	0.12165E+3+0.29220E+1i	−0.10053E+0−0.82002E−2i
	5	0.13521E+2	0.20366E+3+0.43030E+1i	0.73444E−1+0.75855E−2i
8.5E−3	1	0.98063E+0	0.10227E+1+0.48803E+0i	0.11334E+1+0.44985E−1i
	2	0.35343E+1	0.15775E+2+0.20813E+1i	−0.17891E+0−0.69884E−1i
	3	0.65046E+1	0.50599E+2+0.32368E+1i	0.67147E−1+0.37863E−1i
	4	0.95765E+1	0.10639E+3+0.40744E+1i	−0.34546E−1−0.23050E−1i
	5	0.12681E+2	0.18335E+3+0.47324E+1i	0.21095E−1+0.15250E−1i
0.1	1	0.60357E+0	0.43278E+0+0.45360E+0i	0.10605E+1+0.50290E−1i
	2	0.32682E+1	0.13440E+2+0.13660E+1i	−0.76115E−1−0.66599E−1i
	3	0.63486E+1	0.47401E+2+0.17640E+1i	0.22505E−1+0.24319E−1i
	4	0.94687E+1	0.10264E+3+0.20361E+1i	−0.10783E−1−0.12475E−1i
	5	0.12599E+2	0.17919E+3+0.22503E+1i	0.63736E−2+0.76321E−2i

a^+	n	M_n	W_n	Q_n
5E−5	1	0.91922E+0−0.94408E−2i	0.53974E−1−0.40280E−1i	0.18002E+1+0.26154E+0i
	2	0.50637E−1+0.34453E−2i	0.35818E−1−0.23634E−1i	0.11355E+1+0.23269E+0i
	3	0.13948E−1+0.16353E−2i	0.29776E−1−0.17825E−1i	0.90915E+0+0.22826E+0i
	4	0.59816E−2+0.96030E−3i	0.26331E−1−0.14385E−1i	0.77765E+0+0.22816E+0i
	5	0.31675E−2+0.63539E−3i	0.23960E−1−0.11977E−1i	0.68637E+0+0.22887E+0i
8.5E−3	1	0.98052E+0−0.20764E−1i	0.47453E+0−0.21637E+0i	0.10119E+1+0.37886E+0i
	2	0.17043E−1+0.15826E−1i	0.17763E+0+0.14771E−1i	0.23842E+0+0.28203E+0i
	3	0.18285E−2+0.31139E−2i	0.84145E−1+0.27408E−1i	0.83015E−1+0.16348E+0i
	4	0.39229E−3+0.95508E−3i	0.48291E−1+0.22347E−1i	0.37942E−1+0.10351E+0i
	5	0.12265E−3+0.38477E−3i	0.31432E−1+0.17316E−1i	0.20634E−1+0.71430E−1i
0.1	1	0.99943E+0−0.71601E−2i	0.78885E+0−0.18882E+0i	0.43223E+0+0.35591E+0i
	2	0.67388E−3+0.62272E−2i	0.97669E−1+0.68310E−1i	0.30167E−2+0.82216E−1i
	3	−0.57453E−4+0.65202E−3i	0.32198E−1+0.30275E−1i	−0.32768E−2+0.30331E−1i
	4	−0.24369E−4+0.15926E−3i	0.16376E−1+0.17070E−1i	−0.25877E−2+0.16122E−1i
	5	−0.10629E−4+0.57459E−4i	0.10105E−1+0.11107E−1i	−0.19130E−2+0.10187E−1i

After integrating equation (1a) from $r^+ = 0$ to $r^+ = 1$, an energy balance is obtained as equation (18a), therefore, the system of equations (1) becomes:

Fluid region

$$\frac{\partial T_b^+}{\partial t^+} + \frac{\partial T_b^+}{\partial x^+} = \frac{Nu}{2^{2-2m}}\left(\theta|_{r^+=1} - T_b^+\right), \quad x^+ > 0, \ t^+ > 0 \tag{18a}$$

$$T_b^+(0) = \sin\left(\Omega t^+\right), \quad \text{at } x^+ = 0; \ t^+ > 0 \tag{18b}$$

Solid region

$$I\frac{\partial \theta}{\partial t^+} = \frac{1}{r^{+m}}\frac{\partial}{\partial r^+}\left(r^{+m}\frac{\partial \theta}{\partial r^+}\right), \quad 1 < r^+ < r_2^+; \ x^+ > 0; \ t^+ > 0 \tag{18c}$$

$$-\frac{\partial \theta}{\partial r^+} = Bi_{ext}\theta, \quad \text{at } r^+ = r_2^+; \ x^+ > 0; \ t^+ > 0 \tag{18d}$$

Fluid–solid interface

$$\frac{\partial \theta}{\partial r^+} = Bi_{int}\left(\theta - T_b^+\right), \quad \text{at } r^+ = 1; \ x^+ > 0. \tag{18e}$$

where the Nusselt and Biot numbers are given respectively by:

$$Nu = 2^{2-m}\frac{h_{int}R_1}{k_f} \quad \text{and} \quad Bi_{int} = \frac{Nu}{\gamma 2^{2-m}}. \tag{19}$$

The periodic solutions for T_b^+ and θ can then write as:

$$T_b^+\left(x^+, t^+\right) = \tilde{T}_b^+\left(x^+\right)\exp\left(i\Omega t^+\right) \tag{20}$$

$$\theta\left(x^+, r^+, t^+\right) = \tilde{\theta}\left(x^+, r^+\right)\exp\left(i\Omega t^+\right).$$

Then, the system of equations (18) becomes:

Fluid region

$$i\Omega\tilde{T}_b^+ + \frac{\partial \tilde{T}_b^+}{\partial x^+} = \frac{Nu}{2^{2-2m}}\left(\tilde{\theta}|_{r^+=1} - \tilde{T}_b^+\right), \quad 0 < r^+ < 1; \ x^+ > 0 \tag{21a}$$

$$\tilde{T}_b^+(0) = 1, \quad \text{at } x^+ = 0 \tag{21b}$$

Solid region

$$2i\left(\frac{\beta}{r_2^+ - 1}\right)^2\tilde{\theta} = \frac{1}{r^{+m}}\frac{\partial}{\partial r^+}\left(r^{+m}\frac{\partial \tilde{\theta}}{\partial r^+}\right), \quad 1 < r^+ < r_2^+; \ x^+ > 0 \tag{21c}$$

$$-\frac{\partial \tilde{\theta}}{\partial r^+} = Bi_{ext}\tilde{\theta}, \quad \text{at } r^+ = r_2^+; \ x^+ > 0 \tag{21d}$$

Fluid–solid interface

$$\frac{\partial \tilde{\theta}}{\partial r^+} = Bi_{int}\left(\tilde{\theta} - \tilde{T}_b^+\right), \quad \text{at } r^+ = 1; \ x^+ > 0. \tag{21e}$$

Table 2
The first five coefficients and eigenvalues for a circular tube for different a^+ at $Bi_{ext} = 0.0$ and $\Omega = 0.1$.

a^+	n	λ_n	μ_n	G_n
5E−5	1	0.27046E+1	0.46462E+1+0.53724E+0i	0.14669E+1+0.27581E−1i
	2	0.61312E+1	0.26494E+2+0.18812E+1i	−0.77206E+0−0.75172E−1i
	3	0.94791E+1	0.65488E+2+0.32754E+1i	0.51391E+0+0.82879E−1i
	4	0.12761E+2	0.12118E+3+0.45065E+1i	−0.37653E+0−0.85348E−1i
	5	0.16001E+2	0.19335E+3+0.55719E+1i	0.29147E+0+0.77433E−1i
8.5E−3	1	0.15914E+1	0.22443E+1+0.70169E+0i	0.13359E+1+0.89083E−1i
	2	0.42847E+1	0.16932E+2+0.18464E+1i	−0.50578E+0+0.15527E+0i
	3	0.72842E+1	0.46952E+2+0.26521E+1i	0.27654E+0+0.11982E+0i
	4	0.10363E+2	0.92754E+2+0.32500E+1i	−0.18006E+0+0.90159E−1i
	5	0.13470E+2	0.15445E+3+0.37279E+1i	0.12941E+0+0.70902E−1i
0.1	1	0.12273E+1	0.14427E+1+0.67524E+0i	0.12176E+1+0.93771E−1i
	2	0.40662E+1	0.15057E+2+0.13208E+1i	−0.31199E+0+0.14394E+0i
	3	0.71480E+1	0.44517E+2+0.16506E+1i	0.15019E+0+0.84608E−1i
	4	0.10266E+2	0.89947E+2+0.18856E+1i	−0.93370E−1+0.56362E−1i
	5	0.13394E+2	0.15136E+3+0.20740E+1i	0.65696E−1+0.41247E−1i

a^+	n	M_n	W_n	Q_n
5E−5	1	0.68522E+0−0.34035E−1i	−0.14434E+0+0.73451E−1i	0.74425E+0−0.14805E+1i
	2	0.91546E−1+0.97621E−2i	−0.10361E+0+0.34442E−1i	0.64512E+0−0.91209E+0i
	3	0.30197E−1+0.69862E−2i	−0.77368E−1+0.14285E−1i	0.55104E+0−0.58683E+0i
	4	0.13670E−1+0.44685E−2i	−0.58889E−1+0.42603E−2i	0.45953E+0−0.39217E+0i
	5	0.73952E−2+0.29356E−2i	−0.45917E−1−0.58895E−3i	0.38201E+0−0.27355E+0i
8.5E−3	1	0.94724E+0−0.38318E−1i	0.41147E+0−0.17949E+0i	0.10777E+1+0.26197E+0i
	2	0.42818E−1+0.26554E−1i	0.17403E+0+0.18472E−2i	0.33959E+0+0.26377E+0i
	3	0.66939E−2+0.68579E−2i	0.89621E−1+0.18690E−1i	0.14836E+0+0.17073E+0i
	4	0.18264E−2+0.24033E−2i	0.54248E−1+0.17360E−1i	0.80767E−1+0.11524E+0i
	5	0.68062E−3+0.10472E−2i	0.36548E−1+0.14317E−1i	0.50495E−1+0.82795E−1i
0.1	1	0.98304E+0−0.20648E−1i	0.64046E+0−0.16355E+0i	0.71397E+0+0.27680E+0i
	2	0.14560E−1+0.16461E−1i	0.13608E+0+0.41784E−1i	0.10020E+0+0.13098E+0i
	3	0.16674E−2+0.27005E−2i	0.55354E−1+0.25091E−1i	0.35310E−1+0.60910E−1i
	4	0.41698E−3+0.78695E−3i	0.30621E−1+0.15882E−1i	0.18186E−1+0.35583E−1i
	5	0.15158E−3+0.31159E−3i	0.19756E−1+0.10985E−1i	0.11236E−1+0.23653E−1i

The bulk temperature distribution is obtained as:

$$\tilde{T}_b\left(x^+\right) = \exp\left(-\int_0^{x^+} \sigma \, dx^+\right), \tag{22a}$$

$$\text{with}: \sigma = i\Omega + \frac{Nu}{2^{2-2m}}\left(1 - \psi\left(r^+ = 1\right)\right). \tag{22b}$$

By posing $\sigma = \eta + i\xi$, the bulk temperature is written:

$$\tilde{T}_b^+\left(x^+\right) = \exp\left(-\eta x^+\right)\exp\left(-i\xi x^+\right), \tag{22c}$$

$$\text{where } \left|\tilde{T}_b^+\left(x^+\right)\right| = \exp\left(-\eta x^+\right) \text{ and } \phi_b = -\arg\tilde{T}_b^+\left(x^+\right) = \xi x^+. \tag{22d}$$

The special and temporal distributions on bulk temperature can be expressed as:

$$T_b^+\left(x^+, t^+\right) = A_b\left(x^+\right)\sin\left[\Omega t^+ - \phi_b\left(x^+\right)\right] \tag{22e}$$

The temperature distribution in the solid is expressed by:

$$\tilde{\theta}\left(x^+, r^+\right) = \tilde{T}_b^+\left(x^+\right)\Psi\left(r^+\right), \tag{23}$$

where the function $\Psi(r^+)$ is given for the parallel -plates ($m = 0$) as:

$$\Psi\left(r^+\right) = \varphi(Bi_{int}, \beta)\left[\cos\left(\frac{\tilde{\beta} r^+}{r_2^+ - 1}\right) + \frac{G}{F}\sin\left(\frac{\tilde{\beta} r^+}{r_2^+ - 1}\right)\right], \tag{24a}$$

$$\text{with}: G = \frac{\tilde{\beta}}{r_2^+ - 1}\sin\left(\frac{\tilde{\beta} r_2^+}{r_2^+ - 1}\right) - Bi_{ext}\cos\left(\frac{\tilde{\beta} r_2^+}{r_2^+ - 1}\right)$$

$$F = \frac{\tilde{\beta}}{r_2^+ - 1}\cos\left(\frac{\tilde{\beta} r_2^+}{r_2^+ - 1}\right) + Bi_{ext}\sin\left(\frac{\tilde{\beta} r_2^+}{r_2^+ - 1}\right)$$

$$\varphi(Bi_{int}, \beta) = \frac{Bi_{int}}{\sin\left(\frac{\tilde{\beta}}{r_2^+ - 1}\right)\left[\frac{\tilde{\beta}}{r_2^+ - 1} + Bi_{int}\frac{G}{F}\right] + \cos\left(\frac{\tilde{\beta}}{r_2^+ - 1}\right)\left[Bi_{int} - \frac{\tilde{\beta}}{r_2^+ - 1}\frac{G}{F}\right]}. \tag{24b}$$

For the cylindrical ducts ($m = 1$):

$$\Psi\left(r^+\right) = \varphi(Bi_{int}, \beta)\left[J_0\left(\frac{\tilde{\beta} r^+}{r_2^+ - 1}\right) + \frac{G}{F}Y_0\left(\frac{\tilde{\beta} r^+}{r_2^+ - 1}\right)\right], \tag{24c}$$

$$\text{with}: G = \frac{\tilde{\beta}}{r_2^+ - 1}J_1\left(\frac{\tilde{\beta} r_2^+}{r_2^+ - 1}\right) - Bi_{ext}J_0\left(\frac{\tilde{\beta} r_2^+}{r_2^+ - 1}\right),$$

Table 3
Comparison of the ten eigenvalues and coefficients with the values given by Kim and Ozisik [9] for parallel-plate channel; at $Bi_{ext} = 0.0$ and $a^+ = 0.001$.

b^+	n	M_n by Kim and Ozisik [9]	M_n (present study)	μ_n by Kim and. Ozisik [9]	μ_n (present study)
2	1	0.10025E+1−0.49298E−1i	0.10037E+1−0.50454E−1i	0.10495E+1+0.98404E+0i	0.10498E+1+0.10077E+1i
	2	0.35413E−2+0.43261E−1i	0.27086E−2+0.44537E−1i	0.14694E+2+0.46140E+1i	0.14636E+2+0.47089E+1i
	3	−0.37603E−2+0.47722E−2i	−0.40243E−2+0.47231E−2i	0.47956E+2+0.64429E+1i	0.47833E+2+0.65326E+1i
	4	−0.12425E−2+0.85852E−3i	−0.12959E−2+0.81770E−3i	0.10271E+3+0.74640E+1i	0.10256E+3+0.75412E+1i
	5	−0.48364E−3+0.23924E−3i	−0.49886E−3+0.22112E−3i	0.17893E+3+0.82196E+1i	0.17876E+3+0.82907E+1i
	6	−0.22370E−3+0.88017E−4i	−0.22942E−3+0.79311E−4i	0.27656E+3+0.88429E+1i	0.27637E+3+0.89129E+1i
	7	−0.11751E−3+0.38880E−4i	−0.12010E−3+0.34248E−4i	0.39552E+3+0.93828E+1i	0.39535E+3+0.94554E+1i
	8	0.63680E−4+0.19054E−3i	−0.69114E−4+0.16836E−4i	0.53588E+3+0.98647E+1i	0.53569E+3+0.99418E+1i
	9	−0.41930E−4+0.10754E−4i	−0.42713E−4+0.91036E−5i	0.69761E+3+0.10302E+2i	0.69738E+3+0.10386E+2i
	10	−0.27407E−4+0.63661E−5i	−0.27901E−4+0.52944E−5i	0.88064E+3+0.10704E+2i	0.88042E+3+0.10797E+2i
10	1	0.92301E+0−0.31169E−1i	0.91520E+0−0.32877E−1i	0.18465E+1+0.31459E+0i	0.18684E+1+0.33480E+0i
	2	0.54267E−1+0.10653E−1i	0.55626E−1+0.10458E−1i	0.20945E+2+0.23772E+1i	0.21174E+2+0.24932E+1i
	3	0.15375E−1+0.58963E−2i	0.16209E−1+0.59536E−2i	0.60761E+2+0.57261E+1i	0.61313E+2+0.60790E+1i
	4	0.65324E−2+0.38415E−2i	0.71118E−2+0.40131E−2i	0.12111E+3+0.10042E+2i	0.12205E+3+0.10823E+2i
	5	0.32607E−2+0.27437E−2i	0.36711E−2+0.29885E−2i	0.20188E+3+0.15060E+2i	0.20314E+3+0.16494E+2i
	6	0.17201E−2+0.20451E−2i	0.19885E−2+0.23316E−2i	0.30291E+3+0.20496E+2i	0.30440E+3+0.22806E+2i
	7	0.89521E−3+0.15441E−2i	0.10366E−2+0.18361E−2i	0.42426E+3+0.26057E+2i	0.42569E+3+0.29394E+2i
	8	0.42926E−3+0.11608E−2i	0.46597E−3+0.14228E−2i	0.56597E+3+0.31464E+2i	0.56705E+3+0.35851E+2i
	9	0.16654E−3+0.86287E−3i	0.13147E−3+0.10707E−2i	0.72818E+3+0.36506E+2i	0.72865E+3+0.41816E+2i
	10	0.24832E−4+0.63413E−3i	−0.47224E−4+0.78135E−3i	0.91117E+3+0.41062E+2i	0.91081E+3+0.47063E+2i

Table 4
Comparison of the ten eigenvalues and coefficients with the values given by Kim and Ozisik [9] for circular tube; at $Bi_{ext} = 0.0$ and $a^+ = 0.001$.

b^+	n	M_n by Kim and Ozisik [9]	M_n (present study)	μ_n by Kim and. Ozisik [9]	μ_n (present study)
2	1	0.10152E+1−0.10925E+0i	0.10170E+1−0.11083E+0i	0.22092E+1+0.20035E+1i	0.22120E+1+0.20319E+1i
	2	0.33093E−4+0.96444E−1i	−0.13182E−2+0.98236E−1i	0.14959E+2+0.49448E+1i	0.14914E+2+0.50032E+1i
	3	−0.95922E−2+0.10060E−1i	−0.99431E−2+0.99399E−2i	0.43418E+2+0.58603E+1i	0.43348E+2+0.59022E+1i
	4	−0.30442E−2+0.18357E−2i	−0.31115E−2+0.17714E−2i	0.88317E+2+0.64094E+1i	0.88234E+2+0.64430E+1i
	5	−0.11908E−2+0.52695E−3i	−0.12101E−2+0.49919E−3i	0.14935E+3+0.68613E+1i	0.14927E+3+0.68914E+1i
	6	−0.55656E−3+0.19894E−3i	−0.56372E−3+0.18530E−3i	0.22648E+3+0.72570E+1i	0.22638E+3+0.72847E+1i
	7	−0.29515E−3+0.89697E−4i	−0.29835E−3+0.82225E−4i	0.31962E+3+0.76115E+1i	0.31953E+3+0.76387E+1i
	8	−0.17158E−3+0.45759E−4i	−0.17318E−3+0.41235E−4i	0.42879E+3+0.79345E+1i	0.42871E+3+0.79614E+1i
	9	−0.10687E−3+0.25554E−4i	−0.10774E−3+0.22666E−4i	0.55401E+3+0.82322E+1i	0.55390E+3+0.82598E+1i
	10	−0.70235E−4+0.15292E−4i	−0.70741E−4+0.13275E−4i	0.69520E+3+0.85086E+1i	0.69510E+3+0.85369E+1i
10	1	0.13119E+1+0.36431E−3i	0.82772E+1−0.60921E−1i	0.36051E+1+0.54019E+0i	0.36268E+1+0.55750E+0i
	2	0.10287E+0+0.13481E−1i	0.10396E+1+0.12874E−1i	0.21901E+2+0.24064E+1i	0.22031E+2+0.24671E+1i
	3	0.35129E−1+0.10718E−1i	3.55896E−1+0.10451E−1i	0.55740E+2+0.52175E+1i	0.56030E+2+0.53834E+1i
	4	0.16096E−1+0.80320E−2i	1.68662E−1+0.80914E−2i	0.10497E+3+0.87739E+1i	0.10545E+3+0.91325E+1i
	5	0.85461E−2+0.62805E−2i	9.15278E−2+0.65118E−2i	0.16931E+3+0.12879E+2i	0.17010E+3+0.13543E+2i
	6	0.47283E−2+0.49921E−2i	5.16343E−2+0.53390E−2i	0.24910E+3+0.17325E+2i	0.24985E+3+0.18393E+2i
	7	0.25571E−2+0.39496E−2i	2.81193E−2+0.43482E−2i	0.34388E+3+0.21847E+2i	0.34460E+3+0.23399E+2i
	8	0.17381E−2+0.22888E−2i	1.35583E−2+0.34490E−2i	0.45383E+3+0.26203E+2i	0.45440E+3+0.28250E+2i
	9	0.50967E−3+0.23250E−2i	4.78016E−3+0.26401E−2i	0.57913E+3+0.30205E+2i	0.57939E+3+0.32682E+2i
	10	0.91533E−4+0.17255E−2i	−7.55772E−5+0.19522E−2i	0.72000E+3+0.33753E+2i	0.71982E+3+0.36534E+2i

Table 5
Behaviour of Nusselt number as a function of axial distance x^+ for various orders (N) in a parallel-plates channel ($a^+ = 8.5E{-}3$; $Bi_{ext} = 0.0$ and $\Omega = 0.1$)

a^+	N	$x^+ = 0.2$	$x^+ = 0.4$	$x^+ = 0.6$	$x^+ = 0.8$	$x^+ = 1$
8.5E−3	1	0.60186E+2	0.63009E+2	0.65907E+2	0.68886E+2	0.71956E+2
	2	0.11878E+2	0.11138E+2	0.11105E+2	0.11120E+2	0.11139E+2
	3	0.10186E+2	0.97417E+1	0.97113E+1	0.97157E+1	0.97229E+1
	4	0.96677E+1	0.92694E+1	0.92394E+1	0.92406E+1	0.92444E+1
	5	0.94082E+1	0.90310E+1	0.90011E+1	0.90006E+1	0.90029E+1
	6	0.92522E+1	0.88869E+1	0.88569E+1	0.88558E+1	0.88571E+1
	7	0.91478E+1	0.87902E+1	0.87604E+1	0.87586E+1	0.87592E+1
	8	0.90732E+1	0.87209E+1	0.86911E+1	0.86888E+1	0.86890E+1
	9	0.90170E+1	0.86688E+1	0.86389E+1	0.86364E+1	0.86362E+1
	10	0.89817E+1	0.86359E+1	0.86061E+1	0.86033E+1	0.86030E+1
	15	0.88479E+1	0.85113E+1	0.84815E+1	0.84780E+1	0.84769E+1
	20	0.87878E+1	0.84553E+1	0.84255E+1	0.84217E+1	0.84203E+1
	25	0.87528E+1	0.84226E+1	0.83928E+1	0.83888E+1	0.83872E+1
	30	0.87297E+1	0.84010E+1	0.83712E+1	0.83671E+1	0.83654E+1

$$F = Bi_{ext} Y_0\left(\frac{\tilde{\beta} r_2^+}{r_2^+ - 1}\right) - \frac{\tilde{\beta}}{r_2^+ - 1} Y_1\left(\frac{\tilde{\beta} r_2^+}{r_2^+ - 1}\right)$$

$$\varphi(Bi_{int}, \beta) = \frac{Bi_{int}}{\frac{\tilde{\beta}}{r_2^+ - 1}\left[J_1\left(\frac{\tilde{\beta}}{r_2^+ - 1}\right) + \frac{G}{F} Y_1\left(\frac{\tilde{\beta}}{r_2^+ - 1}\right)\right] + Bi_{int}\left[J_0\left(\frac{\tilde{\beta}}{r_2^+ - 1}\right) + \frac{G}{F} Y_0\left(\frac{\tilde{\beta}}{r_2^+ - 1}\right)\right]}. \quad (24d)$$

5. Results and discussion

Based on the complete solution (CS), we present in Table 1 for fully developed laminar flow between a parallel-plate channel, the first five eigenfunctions G_n, M_n, W_n, Q_n and eigenvalues μ_n and λ_n for different a^+ at $Bi_{ext} = 0$. In Table 2, the same coefficients are listed for circular duct. These values can be used in equations (14) to calculate wall heat flux and temperatures distribution. For comparison purpose with the literature, Tables 3 and 4 show the comparison between the coefficient M_n and the eigenvalues μ_n calculated from GITT model by making use of the subroutine EVLCG from IMSL package and those given by Kim and Ozisik [9] from the Runge–Kutta technique. As it can be seen, the results obtained with these two approaches are in good agreement. In order to facilitate the comparison with literature, numerical values for the parameter a^+ are the same ones as in the refs. [9,10,15,16].

Table 5 shows the convergence of Nusselt number (Nu) as function of the truncating order N. Results obtained indicate that $N = 30$ insure an accuracy of three digits everywhere along the duct. Fig. 2 presents the bulk temperature amplitude distribution for different values of order N. It can be noticed that only few terms ($N = 5$) were necessary. To provide results of high accuracy, five eigenvalues are used for all the cases investigated here.

We study in what follows the influence of transversal heat conduction within the duct wall on two practical cases physically different. The first corresponding to regenerative heat exchangers with sheets of stainless steel and a close spacing of $2R_1 = 10$ mm between the plates [25]. The fluid used is air at low temperature (−50 °C).

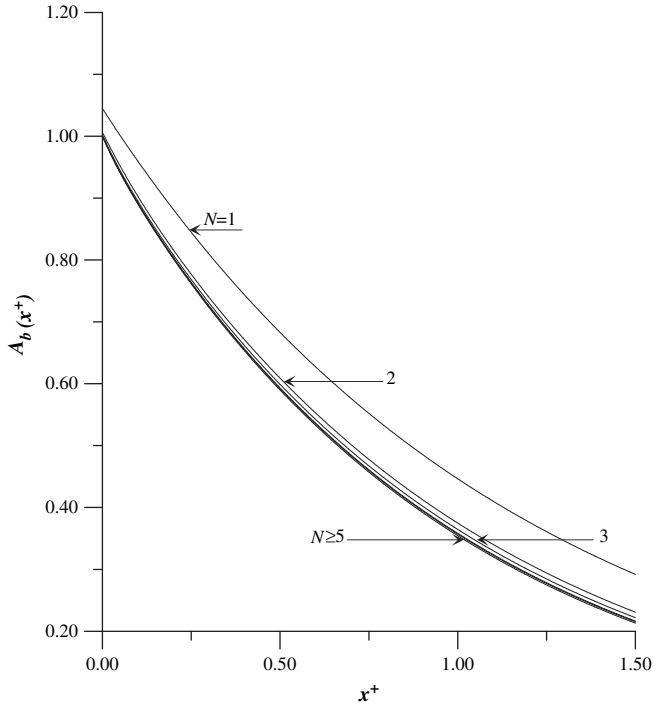

Fig. 2. Amplitude of the bulk temperature as a function of axial distance x^+ for various orders (N) in a parallel-plates channel ($a^+ = 8.5\text{E}{-3}$; $Bi_{ext} = 0.0$ and $\Omega = 0.1$).

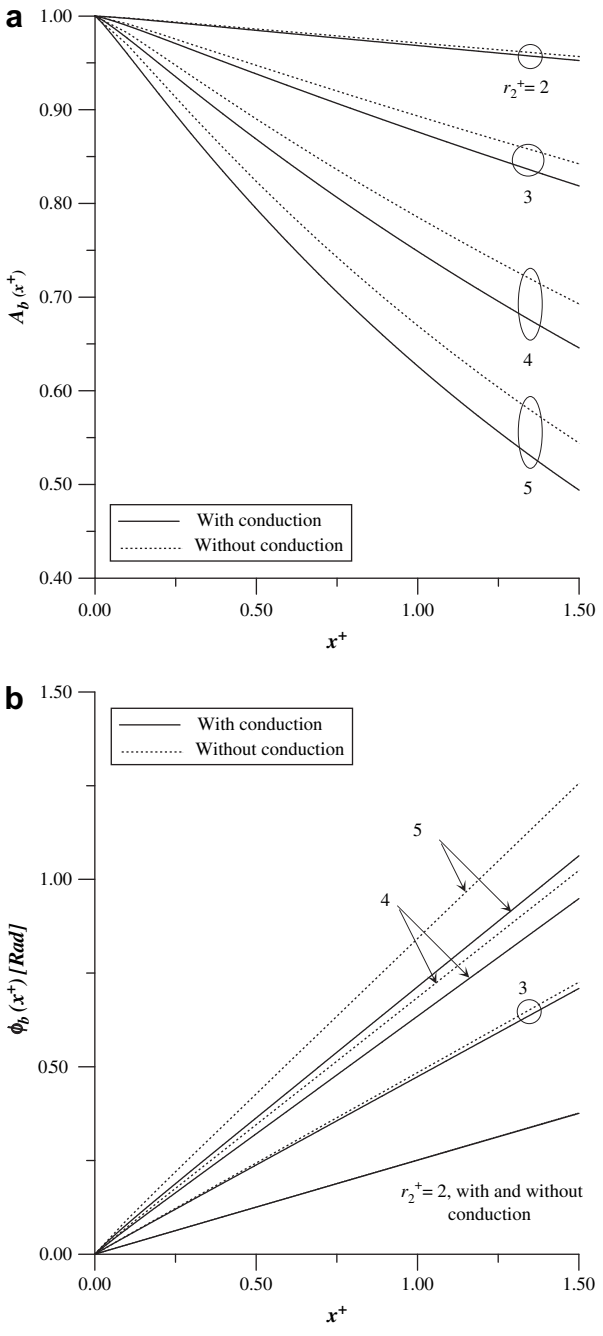

Fig. 3. a. Effects of the thickness wall r_2^+ on the amplitude of the bulk temperature inside parallel-plates for the couple brick/air at $\tau = 4$ h and $Bi_{ext} = 0$. b. Effects of thickness wall r_2^+ on the phase lag of the bulk temperature inside parallel-plates for the couple brick/air at $\tau = 4$ h and $Bi_{ext} = 0$.

In the second case, the system consists of air (at high temperature = 400 °C) flowing inside fireclay brick walls spacing of $2R_1 = 10$ mm [25].

Fig. 3 shows the amplitudes and the phase lags of the bulk temperature along the channel for different r_2^+ ($=R_2/R_1$) by fixing $\tau = 4$ h and $Bi_{ext} = 0$. The particular value of thermal conductivity k_s corresponding to the second case (fireclay brick /air) is 0.36 w m^{-1} K^{-1}. The curves for different r_2^+ represent the effects of the transverse temperature gradients in the solid. For increasing r_2^+, which represent an increase of the wall thickness, the amplitude decays faster along the channel. It can be seen that for large values of r_2^+, (i.e., 5), then the effects of the transverse temperature gradients in the wall are pronounced. The difference of the temperature amplitude with the isothermal wall case (using equation (26a) is substantial. On the other hand, for the small values of r_2^+ (i.e., 2), the two curves (with and without conduction in the wall) are very close to each other.

From Fig. 3b, for increasing values of r_2^+, the difference of the phase lags with the isothermal wall case (thin wall) is substantial and the thin wall model cannot be retained. Fig. 4 shows the amplitudes and the phase lags of the bulk temperature along the channel for different r_2^+ by fixing $\tau = 4$ h and $Bi_{ext} = 0$. The particular value of k_s corresponding to the first case considered (stainless steel/air) is 15 w m^{-1} K^{-1}.

We note that in the same range of values of r_2^+, the curves of the bulk temperature amplitudes and phase lags are confused while considering or disregarding the transverse heat conduction within the wall. In this case, the hypothesis of the "thin wall" can be adopted.

The effect of heat axial conduction within the wall was investigated by Guedes and Cotta [15]. It was observed that for increasing $\beta (= \frac{\delta - 1}{16 P_e^2 K})$, which represents an increase in the wall heat conduction; the amplitudes of the wall temperature are flattened up in the regions very close to the inlet. For increasing values of $a^+ (= \frac{(\rho C)_f}{(\delta - 1)(\rho C)_s} \leq 0.005)$, the effect of the parameter β on the wall temperature and the phase lags becomes less significant. They as also noticed that the amplitude for the bulk temperature is very little influenced by β in the range considered ($\beta = 10^{-7}$–10^{-4}).

Finally, for systems of gases flowing inside a thin metal walls corresponding to large values of $a^+ (>0.005)$, the effects of axial conduction in the wall cannot be neglected in regions close to the inlet but the transverse heat diffusion in the wall can be disregarded.

On the other hand, for small values of a^+ (thick wall with a large thermal capacity), the transverse heat conduction within the duct wall should be considered.

In Figs. 5 and 6, we present the bulk temperature amplitudes and phase lags along the duct respectively for a parallel-plate channel and a circular duct, for both the complete solution (CS) represented by equation (13c) and the QSA evaluated by equation (22c). As given by equation (22d), the bulk temperature amplitude

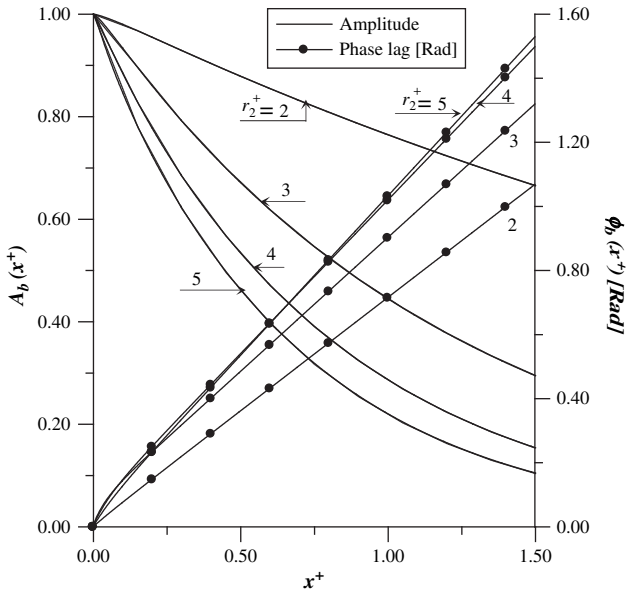

Fig. 4. Effects of thickness wall r_2^+ on the amplitude and phase lag of the bulk temperature inside parallel-plates for the couple stainless steel/air (with and without transversal conduction in the wall) at $\tau = 4$ h and $Bi_{ext} = 0$.

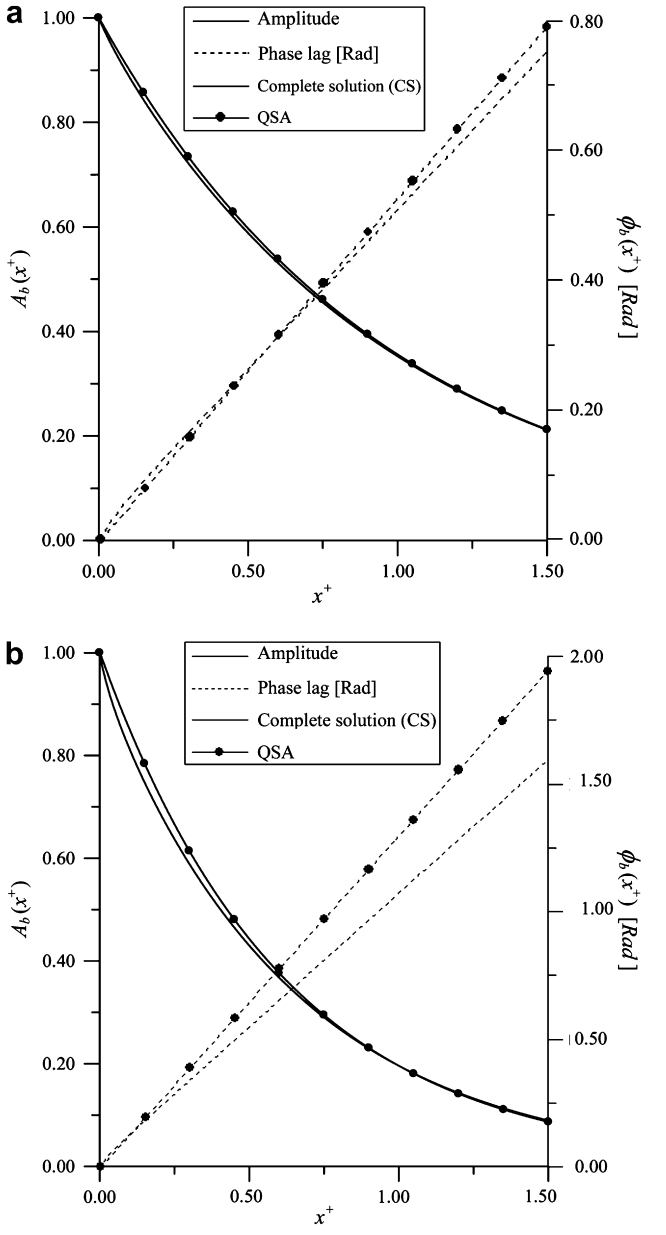

Fig. 5. a. Amplitude and phase lag for bulk temperature as function of axial distance in a parallel-plate channel at $a^+ = 8.5\text{E}{-3}$, $\Omega = 1$. and $Bi_{ext} = 0$. b. Amplitude and phase lag for bulk temperature as function of axial distance in a parallel-plate channel at $a^+ = 8.5\text{E}{-3}$, $\Omega = 1$ and $Bi_{ext} = 0$.

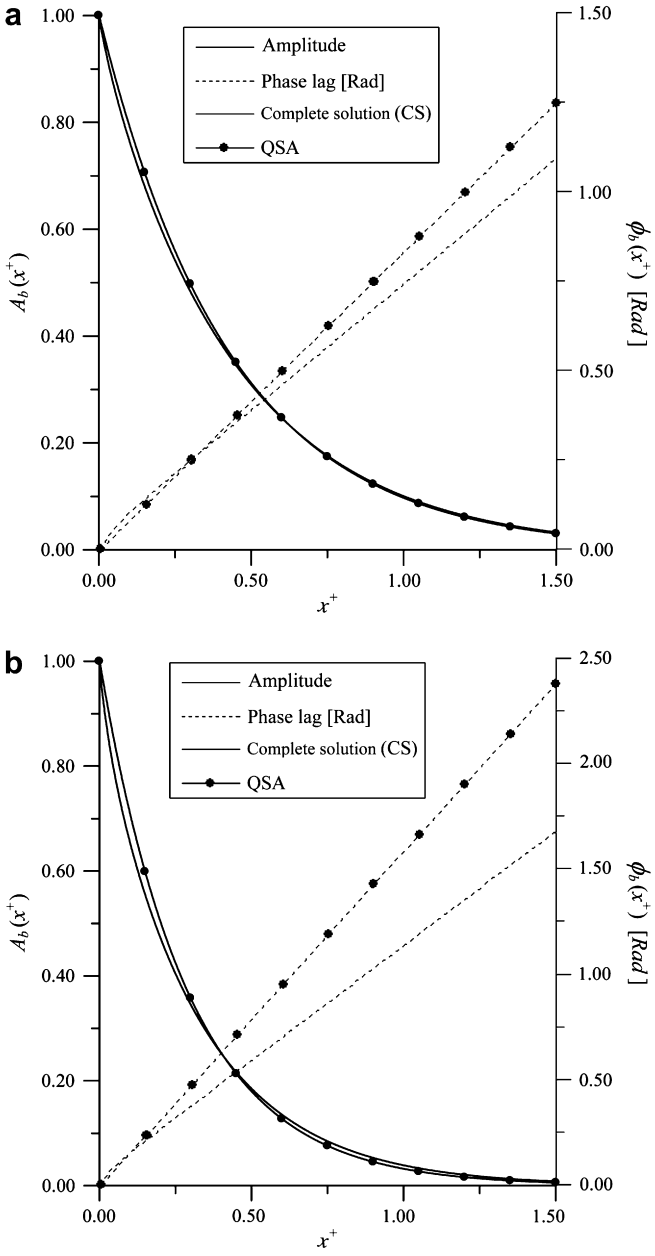

Fig. 6. a. Amplitude and phase lag for bulk temperature as function of axial distance in a circular duct at $a^+ = 8.5\text{E}{-3}$, $\Omega = 0.1$ and $Bi_{ext} = 0$. b. Amplitude and phase lag for bulk temperature as function of axial distance in a circular duct at $a^+ = 8.5\text{E}{-3}$, $\Omega = 1$ and $Bi_{ext} = 0$.

is damped exponentially with the axial distance and the phase lag increases linearly along the ducts.

In most industrial transient heat transfer problems, the thermal design engineer reduces considerably the theoretical analysis by using the quasi-steady approach (QSA) which employs a standard heat transfer coefficient at interface. We will see in what follows if the QSA can approach the CS and examine the effects of the inlet temperature frequency on such approach. From the figures mentioned above, it can be observed that the difference for the phase lag between the quasi-steady approach (QSA) and complete solution (CS) is more significant for larger values of dimensionless inlet frequency Ω and increase with axial distance x^+. Moreover, it is clear that this deviation is more pronounced for a circular duct than a parallel-plate channel for a same physical condition. On the other hand, we note that for the bulk temperature amplitude, these two approaches are equivalent.

Fig. 7a and b shows the damping coefficient η as a function of inlet temperature frequency Ω for both the CS and QSA, respectively for a parallel-plates and circular duct. Note that for lower values of Ω ($\Omega < 0.1$), the results obtained by QSA fit very well with those extracted from CS. On the other hand, for higher values of inlet temperature frequency ($\Omega > 0.1$), the relative deviation is about 2.5% and 3% at $\Omega = 0.5$ respectively for a parallel-plate channel and circular duct. In Fig. 8a and b, we present the phase lag coefficient ξ as function of inlet temperature frequency in parallel-plates and circular duct respectively. We note the similar trends as the

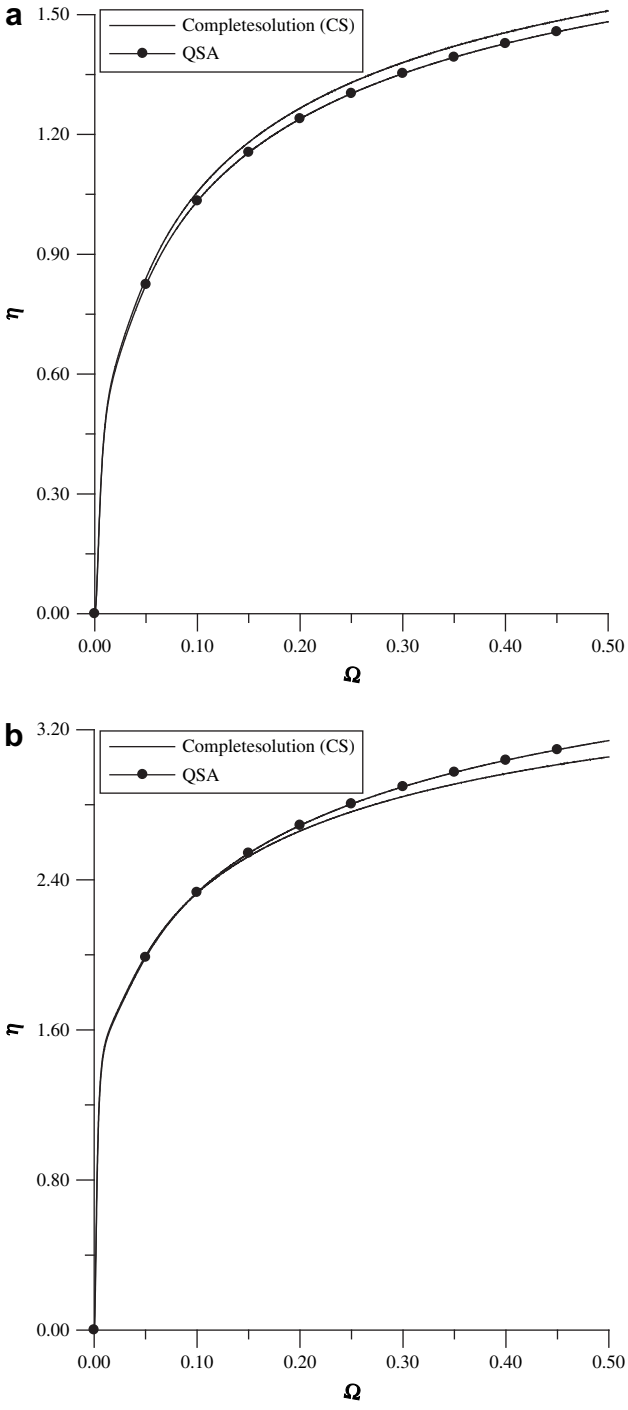

Fig. 7. a. Evolution of the damping coefficient as function of Ω in parallel-plate channel. b. Evolution of the damping coefficient as function of Ω in circular duct.

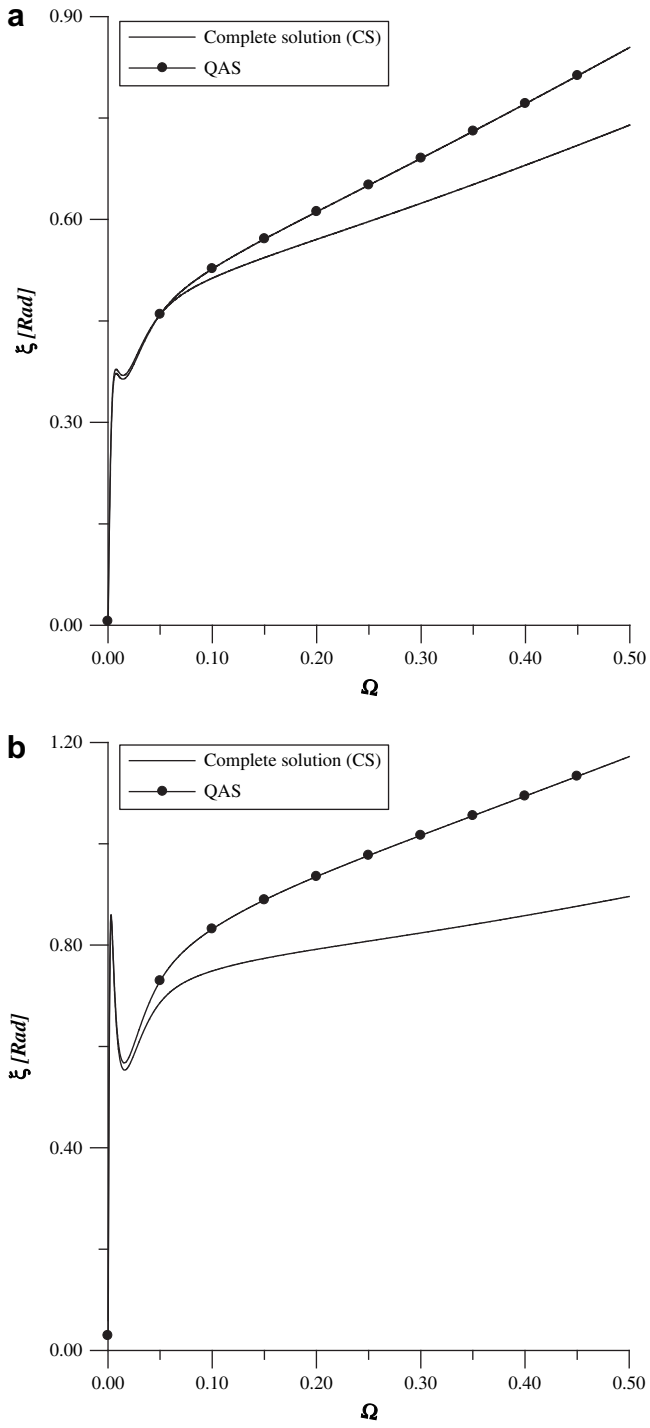

Fig. 8. a. Evolution of the phase lag coefficient as function of Ω in parallel-plate channel. b. Evolution of the phase lag coefficient as function of Ω in circular duct.

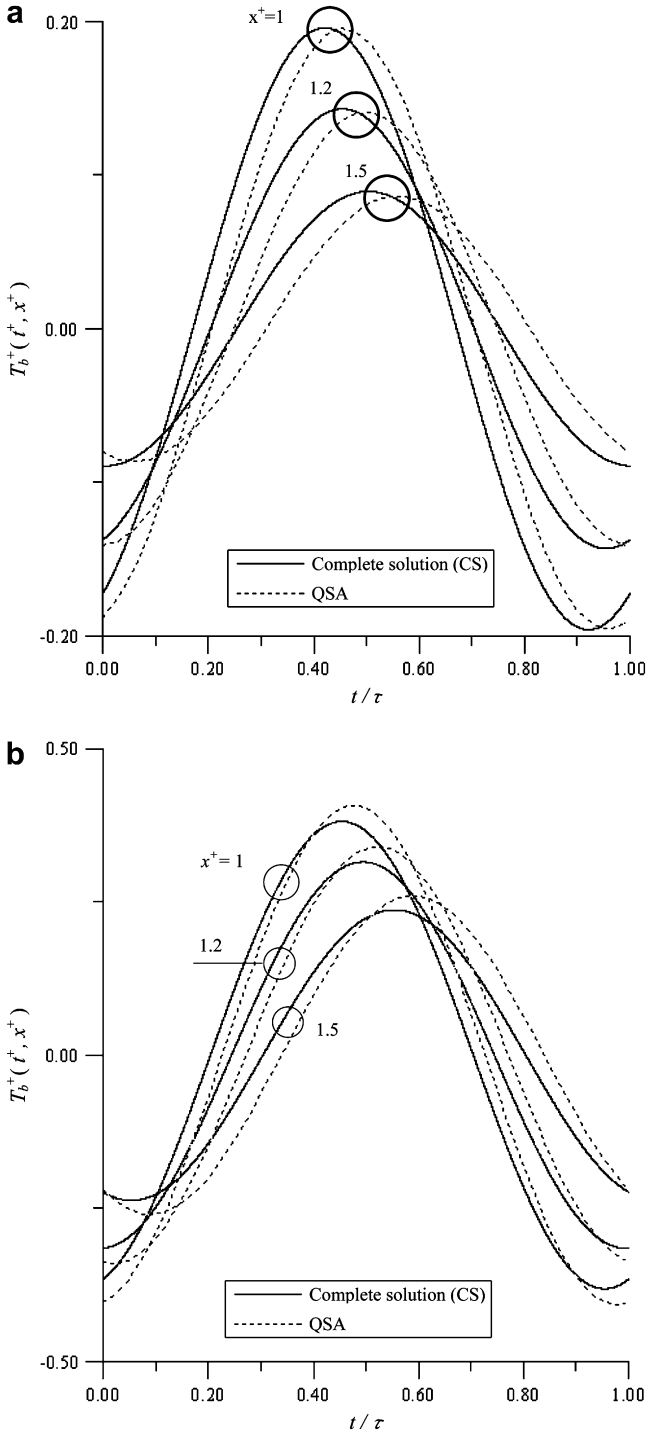

Fig. 9. a. Bulk temperature results on parallel-plate channel for $a^+ = 8.5\text{E}{-3}$, $Bi_{ext} = 0$ and $\Omega = 1$. b. Bulk temperature results on parallel-plate channel for $a^+ = 0.1$, $Bi_{ext} = 0$ and $\Omega = 1$.

damping coefficient η for lower inlet frequency ($\Omega < 0.1$). On the other hand, for higher values of Ω (>0.1), the discrepancy between these two solutions becomes more pronounced and increases with increasing of the inlet frequency. It's estimated at 31% for a circular tube and at 15% for a parallel-plate channel at $\Omega = 0.5$.

The spatial and temporal distributions of the bulk temperature results obtained by QSA and CS are presented in Fig. 9a and b for parallel-plates. Considering a given physical situation characterised by a fixed fluid-to-wall thermal capacitance ratio a^+, these figures reveal that the amplitude of the time wise temperature variation diminishes monotonically with increasing axial distance x^+ from the duct entrance. Moreover, the maxima of the successive curves are displaced in time, indicating an increasing phase lag as the downstream distances. Further inspection of these figures show that decreasing values of the parameter a^+ have a decisive influence both in diminishing the amplitude of the time wise temperature variation and increasing the phase lag.

Finally, in Fig. 10, we present the Nusselt number as function of time on $x^+ = 1$ respectively in the parallel-plates and circular duct

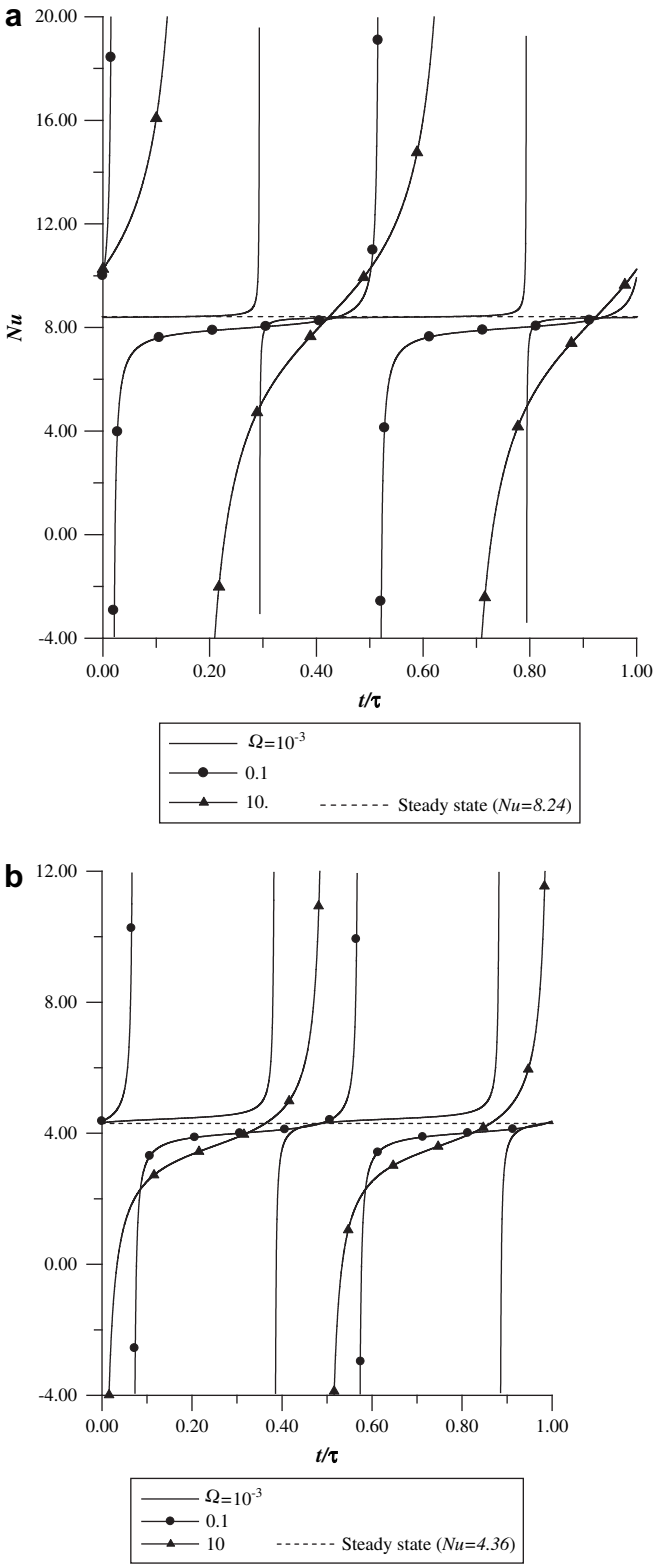

Fig. 10. a. Nusselt number as function of the time on $x^+ = 1$ in parallel-plates. b. Nusselt number as function of the time on $x^+ = 1$ in a circular duct.

for various values of the inlet frequency. When the bulk and wall temperatures are close and the heat flow is not zero, the Nusselt number tends to infinity. When $T_b < T_{r+=1}$, the heat flux from the wall to the fluid and the Nusselt number tends to $+\infty$. When T_b becomes bigger than $T_{r+=1}$, the heat flow changes direction and the Nuselt number tends to $(-\infty)$. In other hand, we remark that for lower inlet frequency ($\Omega = 0.001$) the horizontal portion of the Nusselt number curve is close accord with the know steady state Nusselt number (dashed line) $Nu = 8.25$ and 4.36 respectively for parallel-plate channel and circular duct. For higher inlet frequency ($\Omega = 0.1$–10), the instantaneous Nusselt number will become highly time-dependent and the QSA becomes inadequate.

6. Conclusion

In the present paper, the conjugate heat transfer problem has been studied for the laminar forced convection of a fluid within a parallel-plate channel and a circular duct with periodically varying inlet temperature. Initially, the influence of transversal heat conduction in the duct wall is studied through two practical cases (brick/air and stainless steel/air). It is shown that for small values of a^+(thick wall with a large thermal capacity), the isothermal wall model cannot be retained.

A complete solution (CS) using a Generalized Integral Transform Technique (GITT) is developed and compared with a standard Quasi-steady Approach (QSA) using a constant heat transfer coefficient at fluid–solid interface. These two solutions have displayed a very good agreement for lower frequencies of the inlet temperature. For higher frequencies, the QSA leads to substantial error.

Appendix

The temperature distribution in the duct wall, respectively for a parallel-plate channel and circular duct is required in the form as:

$$\tilde{\theta} = A\cos\left(\tilde{\beta}r^+\right) + B\sin\left(\tilde{\beta}r^+\right) \tag{25a}$$

$$\tilde{\theta} = CJ_0\left(\tilde{\beta}r^+\right) + DY_0\left(\tilde{\beta}r^+\right). \tag{25b}$$

When we substitute equations (25a) and (25b) into equation (4c), we obtain the following equation:

$$\frac{\partial\tilde{T}^+(x^+,1)}{\partial r^+} + \tilde{H}\tilde{T}^+\left(x^+,1\right) = 0. \tag{25c}$$

For parallel-plate channel

$$\tilde{H}=\gamma\frac{\tilde{\beta}}{r_2^+-1}\frac{\sin\left(\frac{\tilde{\beta}}{r_2^+-1}\right)-\left[\frac{\frac{\tilde{\beta}}{r_2^+-1}\sin\left(\frac{\tilde{\beta}r_2^+}{r_2^+-1}\right)-Bi_{ext}\cos\left(\frac{\tilde{\beta}r_2^+}{r_2^+-1}\right)}{Bi_{ext}\sin\left(\frac{\tilde{\beta}r_2^+}{r_2^+-1}\right)+\frac{\tilde{\beta}}{r_2^+-1}\cos\left(\frac{\tilde{\beta}r_2^+}{r_2^+-1}\right)}\right]\cos\left(\frac{\tilde{\beta}}{r_2^+-1}\right)}{\cos\left(\frac{\tilde{\beta}}{r_2^+-1}\right)+\left[\frac{\frac{\tilde{\beta}}{r_2^+-1}\sin\left(\frac{\tilde{\beta}r_2^+}{r_2^+-1}\right)-Bi_{ext}\cos\left(\frac{\tilde{\beta}r_2^+}{r_2^+-1}\right)}{Bi_{ext}\sin\left(\frac{\tilde{\beta}r_2^+}{r_2^+-1}\right)+\frac{\tilde{\beta}}{r_2^+-1}\cos\left(\frac{\tilde{\beta}r_2^+}{r_2^+-1}\right)}\right]\sin\left(\frac{\tilde{\beta}}{r_2^+-1}\right)} \tag{25d}$$

The complex parameter $\tilde{H}$ incorporates the effects of the three parameters that govern the complete conjugated problem, namely γ, β and Biot number Bi. The system of equations (5) may be reduced to those analyzed in literature [7–13] which neglecting the thermal diffusion in the duct walls, if the coupling parameter $\tilde{H}$ is replaced by:

$$\tilde{H}_0 = Bi^+ + ib^+. \tag{26a}$$

This particular case is obtained in present study for small values of $\beta(\sin\beta \approx \beta)$, this condition can be justified only for heat transfer in

flows bounded by extremely thin walls. Then, the parameter $\tilde{H}$ as expressed by:

$$\lim_{\tilde{\beta}\to 0}\tilde{H} = -\gamma\frac{\tilde{\beta}^2\left(r_2^+-1\right)-Bi_{ext}\left(r_2^+-1\right)^2-Bi_{ext}\tilde{\beta}^2 r_2^+}{\left(r_2^+-1\right)^2\left[1+Bi_{ext}\left(r_2^+-1\right)\right]} \tag{26b}$$

Moreover if the duct wall external surface is insulated ($Bi_{ext}\to 0$), then the coefficient $\tilde{H}$ becomes:

$$\lim_{\tilde{\beta}\to 0}\tilde{H} = \tilde{H}_0 = -\frac{\gamma}{r_2^+-1}\left[\tilde{\beta}^2-\left(r_2^+-1\right)Bi_{ext}\right]. \tag{26c}$$

For a circular duct:

$$\tilde{H}=\gamma\frac{\tilde{\beta}}{r_2^+-1}\frac{J_1\left(\frac{\tilde{\beta}}{r_2^+-1}\right)+\left[\frac{\frac{\tilde{\beta}}{r_2^+-1}J_1\left(\frac{\tilde{\beta}r_2^+}{r_2^+-1}\right)-Bi_{ext}J_0\left(\frac{\tilde{\beta}r_2^+}{r_2^+-1}\right)}{Bi_{ext}Y_0\left(\frac{\tilde{\beta}r_2^+}{r_2^+-1}\right)-\frac{\tilde{\beta}}{r_2^+-1}Y_1\left(\frac{\tilde{\beta}r_2^+}{r_2^+-1}\right)}\right]Y_1\left(\frac{\tilde{\beta}}{r_2^+-1}\right)}{J_0\left(\frac{\tilde{\beta}}{r_2^+-1}\right)+\left[\frac{\frac{\tilde{\beta}}{r_2^+-1}J_1\left(\frac{\tilde{\beta}r_2^+}{r_2^+-1}\right)-Bi_{ext}J_0\left(\frac{\tilde{\beta}r_2^+}{r_2^+-1}\right)}{Bi_{ext}Y_0\left(\frac{\tilde{\beta}r_2^+}{r_2^+-1}\right)-\frac{\tilde{\beta}}{r_2^+-1}Y_1\left(\frac{\tilde{\beta}r_2^+}{r_2^+-1}\right)}\right]Y_0\left(\frac{\tilde{\beta}}{r_2^+-1}\right)}. \tag{27a}$$

For the thin wall ($\beta\to 0$), the effects of heat conduction in the wall can be neglected, then:

$$\lim_{\tilde{\beta}\to 0}\tilde{H}=-\gamma\frac{\tilde{\beta}^2\left(r_2^+-1\right)\left(\frac{1}{r_2^+}+1\right)-2Bi_{ext}\left(r_2^+-1\right)^2-Bi_{ext}\tilde{\beta}^2\ln\left(\frac{\tilde{\beta}r_2^+}{r_2^+-1}\right)}{2\left(r_2^+-1\right)^2\left[1+\left(\frac{r_2^+-1}{r_2^+}\right)+Bi_{ext}\ln\left(\frac{\tilde{\beta}r_2^+}{r_2^+-1}\right)-Bi_{ext}\ln\left(\frac{\tilde{\beta}}{r_2^+-1}\right)\right]}. \tag{27b}$$

In addition for a zero surface heat flux ($Bi_{ext}\to 0$), we obtain:

$$\tilde{H} = -\frac{\gamma}{\left(r_2^+-1\right)}\left[\tilde{\beta}^2-Bi_{ext}\left(r_2^+-1\right)\right]. \tag{27c}$$

Appendix. Supplementary data

Supplementary data associated with this article can be found in the online version, at doi:10.1016/j.ijthermalsci.2009.05.012.

References

[1] S. Kakaç, Y. Yener, Exact solution of transient forced convection energy equation for timewise variation of inlet temperature, Int. J. Heat Mass Transfer 16 (1973) 2205–2214.

[2] S. Kakaç, Y. Yener, Frequency response analysis of transient turbulent forced convection for timewise variation of inlet temperature, in: S. Kakaç, D.B. Spalding (Eds.), Hemisphere Publishing Corporation, New York, 1979, pp. 865–880.

[3] R.M. Cotta, M.N. Ozisik, Laminar forced convection inside ducts with periodic variation of inlet temperature, Int. J. Heat Mass Transfer 29 (1986) 1445–1501.

[4] W.S. Kim, M.N. Ozisik, Turbulent forced convection inside a parallel-plate channel with periodic variation of inlet temperature, Trans. ASME J. Heat Transfer 111 (1989) 882–888.

[5] M. Arik, C.A.C. Santos, S. Kakaç, Turbulent forced convection with sinusoidal variation of inlet temperature between two parallel-plates, Int. Comm. Heat Mass Transfer 23 (1996) 1121–1132.

[6] M. Unsal, A solution for the complex eigenvalues and eigenfunctions of the periodic Graetz problem, Int. Comm. Heat Mass Transfer 25 (1998) 585–592.

[7] E.M. Sparrow, F.N. Farias, Unsteady heat transfer in ducts with time varying inlet temperature and participating walls, Int. J. Heat Mass Transfer 11 (1968) 837–853.

[8] R.M. Cotta, M.D. Mikhailov, M.N. Ozisik, Transient conjugated forced convection in ducts with periodically varying inlet temperature, Int. J. Heat Mass Transfer 30 (1987) 2073–2082.

[9] W.S. Kim, M.N. Ozisik, Conjugated laminar forced convection in ducts with periodic variation of inlet temperature, Int. J. Heat Fluid Flow 11 (1990) 311–320.

[10] J.S. Travelho, F.N. Santos, Solution for transient conjugated forced convection in the thermal entrance region of a duct with periodically varying inlet temperature, Trans. ASME J. Heat Transfer 113 (1991) 558–562.

[11] J.S. Travelho, F.N. Santos, Unsteady conjugate heat transfer in a circular duct with convection from the ambient and periodically varying inlet temperature, Trans. ASME J. Heat Transfer 120 (1998) 506–510.

[12] S. Kakaç, W. Li, Unsteady turbulent forced convection in a parallel-plate channel with timewise variation of inlet temperature, Int. J. Heat Mass Transfer 37 (1994) 447–456.

[13] W. Li, S. Kakaç, Unsteady thermal entrance heat transfer in laminar flow with a periodic variation of inlet temperature, Int. J. Heat Mass Transfer 34 (1991) 2581–2592.

[14] S. Cheroto, M.D. Mikhailov, S. Kakaç, R.M. Cotta, Periodic laminar forced convection: solution via symbolic computation and integral transforms, Int. J. Thermal Sci. 38 (1999) 613–621.

[15] R.O.C. Guedes, R.M. Cotta, Periodic laminar forced convection within ducts including wall heat conduction effects, Int. J. Eng. Sci. 29 (1991) 535–547.

[16] R.O.C. Guedes, M.N. Ozisik, R.M. Cotta, Conjugated periodic turbulent forced convection in a parallel-plate channel, Trans. ASME J. Heat Transfer 116 (1994) 40–46.

[17] B. Fourcher, K. Mansouri, An approximate analytical solution to the Graetz problem with periodic inlet temperature, Int. J. Heat Fluid Flow 18 (1997) 229–235.

[18] K. Mansouri, D. Sadaoui, B. Fourcher, The effects of inlet temperature frequency on the quasi-steady approach of periodic conjugated heat transfer problem, Int. J. Eng. Sci. 42 (2004) 825–839.

[19] F.V. Castellões, R.M. Cotta, Analysis of transient and periodic convection in microchannels via integral transforms, Prog. Comput. Fluid Dynamics 6 (2006) 321–326.

[20] G.D. Ngoma, F. Erchiqui, Heat transfer and slip effects on liquid flow in a micro channel, Int. J. Thermal Sci. 46 (2007) 1076–1083.

[21] W. Sun, S. Kakaç, A.G. Yazicioglu, A numerical study of single phase convective heat transfer in micro tubes for slip flow, Int. J. Thermal Sci. 46 (2007) 2581–2592.

[22] J. Peixinho, C. Desaubry, M. Lebouché, Heat transfer of non-Newtonian fluid (Carbopol aqueous solution) in transitional pipe flow, Int. J. Heat Mass Transfer 51 (2008) 198–209.

[23] F. Tamisli, Laminar flow of a non-Newtonian fluid in channels with wall suction or injection, Int. J. Eng. Sci. 44 (2006) 650–661.

[24] O. Jambal, T. Shigechi, G. Davaa, S. Momki, Effects of viscous dissipation and fluid axial heat convection on heat transfer for non-Newtonian fluids in ducts with uniform wall temperature, Int. Comm. Heat Mass Transfer 32 (2005) 1165–1173.

[25] M. Jakob, Heat Transfer, vol. 2, New York, London: Wiley & Sons, Inc.